Journal of Zhejiang University-SCIENCE A (Applied Physics & Engineering) *2022 23(12):974-987*
www.jzus.zju.edu.cn; www.springer.com/journal/11582
E-mail: jzus_a@zju.edu.cn

Research Article

https://doi.org/10.1631/jzus.A2200233

Hole-growth phenomenon during pyrolysis of a cation-exchange resin particle

Zheng-liang HUANG[1], Yun-bo YU[1], Qi SONG[1], Yao YANG[1]✉, Jing-yuan SUN[1], Jing-dai WANG[2], Yong-rong YANG[2]

[1]*Zhejiang Provincial Key Laboratory of Advanced Chemical Engineering Manufacture Technology, College of Chemical and Biological Engineering, Zhejiang University, Hangzhou 310027, China*
[2]*State Key Laboratory of Chemical Engineering, College of Chemical and Biological Engineering, Zhejiang University, Hangzhou 310027, China*

Abstract: A novel central hole-expansion phenomenon is identified, in which the cation-exchange resin is pyrolyzed in a mixed atmosphere of nitrogen and oxygen at 400–500 ℃. In this reaction, the reaction path is predictable and always starts from the center of the resin particle to form a central hole, then continues and expands around the hole, finally forming a uniformly distributed hole group; the particle surface remains intact. Analysis shows that this formation mode is due to the different reaction paths of sulfonic groups between the surface and interior of the particle, caused by the temperature difference. On the surface, transformation reactions happen at high temperatures (410–500 ℃) to form stable organic sulfur structures, while decomposition occurs inside the particle at a relatively low temperature (<410 ℃) and promotes complete pyrolysis of the copolymer matrix to form holes.

Key words: Non-catalytic gas-solid reaction; Cation-exchange resin; Pyrolysis; Central-hole expansion; Temperature difference; Transformation

1 Introduction

Non-catalytic gas-solid reactions, such as those evident in reduction of iron ore, calcination of limestone, coal gasification, biomass pyrolysis, and reprocessing of nuclear waste fuels are an important class of chemical reactions in chemical engineering, metallurgy, nuclear energy, and other industries. For nearly a century, scholars (Yagi and Kunii, 1955; Petersen, 1957; Wen, 1968; Szekely and Propster, 1975; Ramachandran and Doraiswamy, 1982) have proposed different reaction models to describe non-catalytic gas-solid reactions. Yagi and Kunii (1955) proposed the sharp-interface model. They believed that for non-porous solids, the reaction started from the solid surface and gradually proceeded to the interior of the solid reactant, accompanied by shrinking of the solid volume during the reaction. Petersen (1957) proposed the pore model and hypothesized that for a porous solid, the gas first reacted with the pore wall when it diffused into the solid reactant through the pores. Wen (1968) proposed the zone-reaction model and believed that the reaction occurred in a region with a certain thickness inside the solid reactant and that the gas reacted with the solid while diffusing into its interior. When the reaction rate is much lower than the diffusion rate, the gas concentration inside the solid reactant is uniform. Thus, the reaction can be regarded as proceeding throughout the entire solid volume, which develops into the volume-reaction model (Ramachandran and Doraiswamy, 1982). Szekely and Propster (1975) proposed the grain model, with a solid particle being made up of many grains. In this model, the gas diffuses into the solid through the space among the grains and reacts with them. The reaction processes described by the above four models can be divided into two types. One is the shrinking-core model, in which the reaction proceeds from the outside to the inside

✉ Yao YANG, yao_yang@zju.edu.cn
Yao YANG, https://orcid.org/0000-0003-3611-2859

Received Apr. 25, 2022; Revision accepted Aug. 29, 2022; Crosschecked Oct. 16, 2022

of the solid reactant. The other type includes the pore model, zone reaction model, and grain model, in which the gas enters the interior of the solid reactant through pore channels and causes simultaneous internal and external reactions. This type of reaction process is random, and it is difficult to determine the site and direction of the reaction in a solid. In recent years, scholars have developed a series of modified reaction models (based on the above classic models) for different specific reaction processes (Uhde and Hoffmann, 1997; Yoshioka et al., 2001; Homma et al., 2005; Safari et al., 2009; Sadhukhan et al., 2010). These models complement research on non-catalytic gas-solid reactions to a certain degree.

In this study, we investigated the pyrolysis process of cation-exchange resins in a tube furnace reactor under different conditions. We believe we identified a new type of reaction, which we call the central-hole expansion mode, and which is entirely different from the traditional non-catalytic gas-solid reaction models reported. To further explore this reaction mode, the influence laws of reaction atmosphere, reaction temperature, and resin structure on the new pyrolysis mode were studied. In addition, the formation mechanism of the central-hole expansion mode was preliminarily investigated from the aspect of the decomposition and transformation of sulfonic groups. The proposed central-hole expansion mode may provide guidance for the verification and development of non-catalytic gas-solid reaction models due to its regular reaction process and predictable reaction sites.

2 Experimental

2.1 Materials

Table 1 lists the resins used in this study. An example of resin structure is shown in Fig. S1 of the electronic supplementary materials (ESM). Before use, cation-exchange resins were pretreated as follows: the resins were soaked in the saturated saline for 24 h to remove soluble impurities, and then in 1-mol/L hydrochloric acid solution for 5 h and 1-mol/L sodium hydroxide solution for 5 h in sequence. Finally, the resins were washed to be neutral and dried to obtain Na-type cation-exchange resins. After all the above, the dried resins were put into CsCl or $Co(NO_3)_2$ solution to be continuously shaken in a thermostatic water-bath oscillator for 48 h at 25 ℃ and 200 r/min. Then, Cs^+- or Co^{2+}-doped cation-exchange resins were prepared after ion exchange, at a concentration of 30 g/L.

2.2 Experimental methods

The experimental apparatus used for pyrolysis of the cation-exchange resins is shown in Fig. S2 of the ESM. In the experiment, the reaction temperature was between 300 and 520 ℃. The reaction atmosphere was nitrogen or a nitrogen-oxygen mixture (N_2 (0% O_2 in volume), 3% O_2, 5% O_2, and 10% O_2), and the gas-flow rate was 300 mL/min. The temperature and atmosphere in the tube furnace reactor were first adjusted to the required conditions. When the reaction condition was stable, the dried cation-exchange resins were dispersed in small crucibles (10.0 mm×10.0 mm×5.5 mm) to avoid the mutual contact between particles. Then the small crucibles were placed into a large crucible (100 mm×20 mm×20 mm), and the large crucible was put directly into the tube furnace for resin pyrolysis. The reaction time was from 5 to 30 min. After reaction, the large crucible was taken out immediately and cooled. The pyrolyzed products were cut in half along the central axis using a blade with a thickness of 0.1 mm. After this, we analyzed the surface and internal morphologies, element distribution, and functional-group information.

2.3 Characterization methods

Morphologies of the pyrolysis products were characterized with a scanning electron microscope (SEM) (SU-3500, Hitachi, Japan) with an acceleration voltage

Table 1 Resins used in this study

Resin	Specification	Crosslinking degree (in weight) (%)	Average particle size (μm)
Cation-exchange resins	IRN-97H	10	400
	IRN-120	7	400
	D001	7	400
	001×7	7	900
Polystyrene-divinylbenzene resin bead	St-DVB	2	400

of 5.0 kV and emission current of 110 μA. We used an energy dispersive spectrometer (EDS) (X-Max 20, Oxford Instruments, UK) in conjunction with the SEM to analyze the element distribution on the surface and interior of the raw resin (Trubetskaya et al., 2019). Thermogravimetric (TG) curves and derivative thermogravimetric (DTG) curves of cation-exchange resins were obtained with a thermogravimetric analyzer (TGA) (TGA/DSC 3+, Mettler Toledo, Switzerland). The resins were heated from 30 to 850 °C at a heating rate of 10 °C/min in the flowing N_2 (0%-O_2) or 3%-O_2 atmospheres. The sulfur speciation on the surface of pyrolysis products was investigated with an X-ray photoelectron spectrometer (XPS) (ESCALAB 250Xi, Thermo Fisher Scientific, USA) with an Al-Kα light source (Bava et al., 2019). The gas inside the pyrolysis products was adsorbed by KOH solution and then analyzed with ion chromatography (ICS-90, DIONEX, USA). The chromatograph was equipped with a conductivity detector, a Dionex Ion Pac AG14 guard column (50 mm×4 mm I.D. (inside diameter)), and a Dionex Ion Pac AS14 separation column (250 mm× 4 mm I.D.). Suppression was achieved with a Dionex AMMS-III (4 mm). Typically, 25-μL samples were injected into the column and eluted with a mixture of Na_2CO_3 and $NaHCO_3$ (0.25 mol/L) at a flow rate of 0.5 mL/min (Chen et al., 2006).

3 Results and discussion

3.1 Discovery of the central-hole expansion mode

Fig. 1 shows the morphological change in doped IRN-97H cation-exchange resins during pyrolysis at 450 °C in a 3%-O_2 atmosphere. At 5 min, there was no significant change in the surface or interior of the particle compared to raw resin. At 10 min, a hole appeared in the center of the particle, but there was no obvious change in the particle surface, indicating that the pyrolysis reaction may have started from the center of the resin particle. As the pyrolysis time increased to 20 min, the number of holes increased, and a circle of evenly arranged small holes appeared around the central hole. As the time further increased to 30 min, the volume of holes inside the resin particle increased, causing the break and collapse of some of the hole walls. In addition, the particle size increased from 400 to 460 μm. However, the surface of the resin particles still remained intact at 30 min. According to statistics, an average of 16 out of 20 resin particles participating in the reaction exhibit the above pyrolysis behavior during the pyrolysis process, and the remaining particles break up.

We suspected that the above phenomenon may have been caused by the non-uniformity of the cation-exchange resins. Therefore, we obtained the distribution

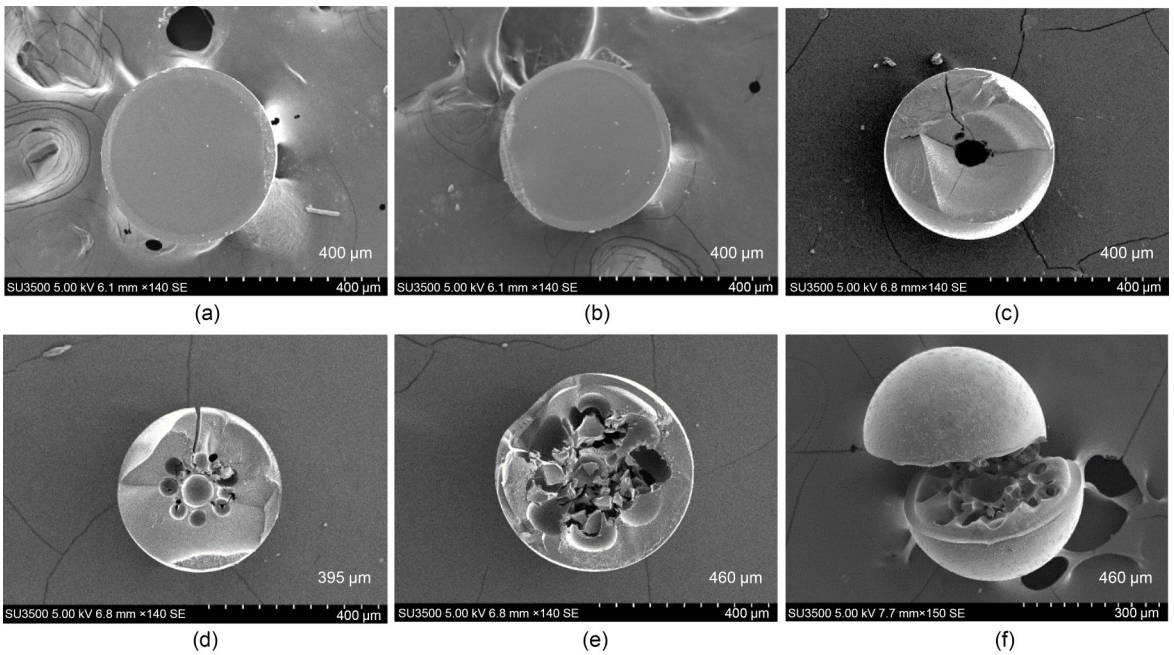

Fig. 1 Morphologies of IRN-97H cation-exchange resins (a) and products pyrolyzed at 450 °C in a 3%-O_2 atmosphere for 5 min (b), 10 min (c), 20 min (d), and 30 min (e and f)

of elements on the surface and interior of the IRN-97H raw resins by SEM-EDS, and the results are shown in Fig. 2. The main constituent elements of both the surface and interior are C, O, S, Na, and a small amount of Cs. The relative contents of each element on the surface and interior of resin particles were not much different, and the elements were uniformly distributed. This preliminarily proved that hole formation was not caused by the non-uniformity of the cation-exchange resins.

Next, the IRN-97H resins were cut into hemispheres and pyrolyzed at 450 °C in a 3%-O_2 atmosphere. The morphologies of the products are presented in Fig. S3 of the ESM. At 10 min, a bulge appeared on the flat surface of the hemispherical resin. Subsequently, the bulge gradually grew, causing the flat surface to burst at 15 min. As the reaction time increased to 20 min, the fracture surface expanded, and the pyrolysis degree of the internal matrix increased. At 30 min, the internal structure of the hemispherical resin expanded to the outside from the fractured surface. The spherical surface of the hemispherical resin particle remained intact, and no fracture appeared. This indicates that the pyrolysis process of the hemispherical resins also started from the interior of the particles, and the phenomenon of pyrolysis starting from the interior was not caused by the non-uniformity of the cation-exchange resins.

The pyrolysis behavior of the cation-exchange resins was not caused by the structural difference between the surface and interior of the resin, and the reaction was significantly different from the existing gas-solid reactions or particle pyrolysis models reported in the literature, which mainly start from the particle surface or phase interface, and in which the reaction sites are anisotropic and random (Yoshioka et al., 2001; Homma et al., 2005; Sadhukhan et al., 2009, 2010; Safari et al., 2009; Oluoti et al., 2014; Yao et al., 2018). However, in our experiments, the reaction always started from the exact center of the spherical particles and then spread uniformly around. The process is predictable. So, we decided to name this pyrolysis behavior the central-hole expansion mode in this paper. Next, it was necessary to investigate the universality of the reaction.

3.2 Factors influencing the central-hole expansion mode

3.2.1 Effect of oxygen content

In the pyrolysis of resin, researchers have found that oxygen can promote the pyrolysis reaction, reduce the solid residual rate, and decrease the organic content in the pyrolysis gas (Shen et al., 2011; Amutio et al., 2012; Ren and Zhao, 2012; Bach et al., 2017). Therefore, we first investigated the effect of oxygen content

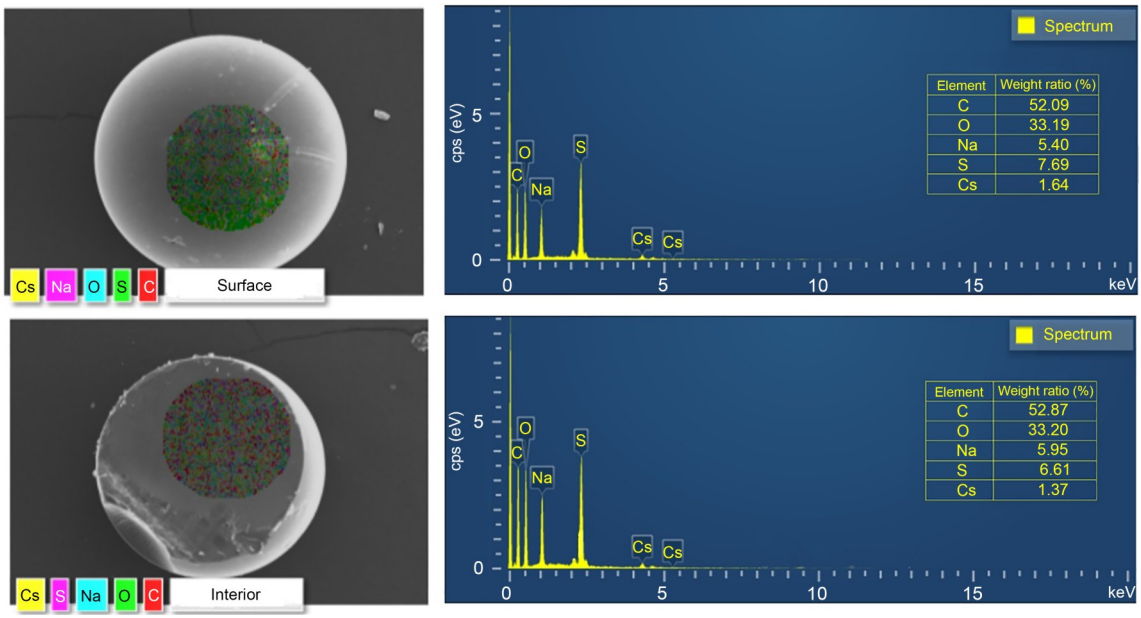

Fig. 2 Distribution of elements on the surface and interior of the IRN-97H raw resin as shown by SEM-EDS. cps represents the counts per second per electron-volt

on the resin pyrolysis behavior. The internal morphologies of the Cs-doped IRN-97H cation-exchange resins pyrolyzed for 30 min in different atmospheres are shown in Fig. 3. In the nitrogen atmosphere, the hole volume inside the particle was small when the resin was pyrolyzed for 30 min. This shows that the holes had not fully grown, and there were still some unreacted resin structures around the holes. As the oxygen content increased, the volume and number of holes inside the resin particles both increased within the same reaction time. In the 10%-O_2 atmosphere, a completely hollow structure was formed in the particles, leaving only a spherical shell. A plausible explanation for this phenomenon is that oxygen can penetrate the resins and react with the organic skeleton, which results in promotion of the pyrolysis reaction.

We collected the particle diameters of resins pyrolyzed in different atmospheres for different times for statistics, and the results are presented in Fig. 4. In the pyrolysis process under nitrogen (0%-O_2) and 3%-O_2 atmospheres, the particle size changed little within 20 min but increased obviously at 30 min. In the pyrolysis process in the 5%-O_2 atmosphere, the particle size gradually increased within 30 min, and the growth rate also gradually increased. The greater the oxygen content was in the reaction atmosphere, the larger the particle size of the products at 30 min. It is possible that the increased gas generated during the formation of holes swells the resin particles and leads to an increase in particle size. This further illustrates that oxygen can promote expansion of holes during the resin pyrolysis process.

3.2.2 Effect of reaction temperature

Reaction temperature (T) is another important factor influencing the pyrolysis process. We conducted pyrolysis of Cs^+-doped IRN-97H cation-exchange resins at different temperatures for 30 min under a 3%-O_2 atmosphere, and the interior structures of typical pyrolysis products are shown in Fig. 5. At 400 ℃, when the reaction time was less than 30 min, the resin particles remained unchanged, with the only one hole being formed in the center of the resin particles. At 450 ℃, when the resin particles were also pyrolyzed for 30 min, there were more and larger holes compared with those in evidence at 400 ℃. When the reaction temperature increased to 500 ℃, the time required to form the hole structure in the resin was shorter. The resin particles formed a hollow structure with fully grown holes in 5 min. After we increased

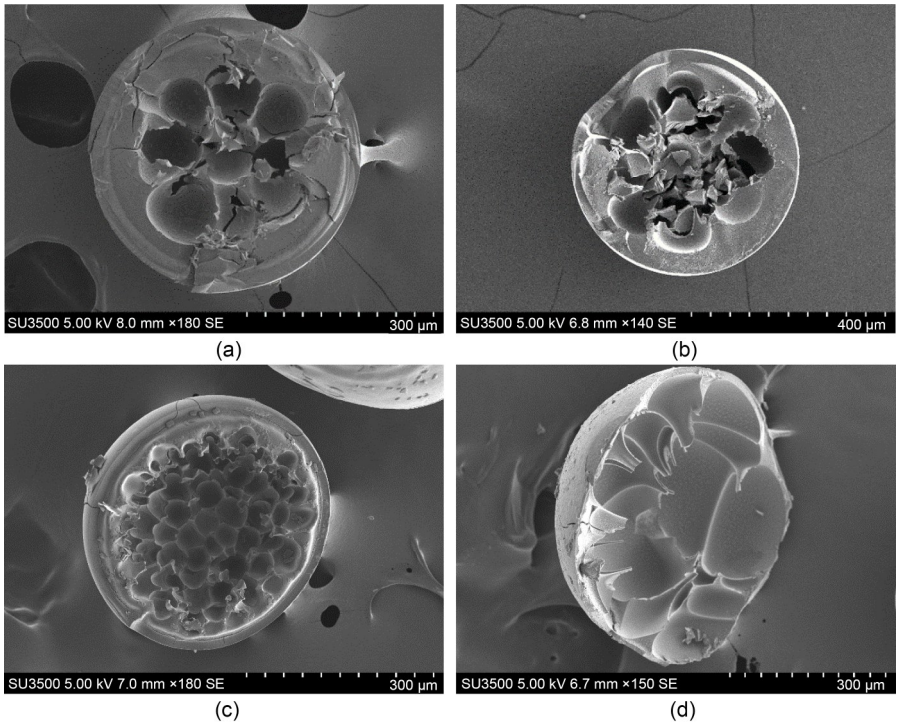

Fig. 3 Internal morphologies of IRN-97H cation-exchange resins pyrolyzed at 450 ℃ for 30 min in N_2 (0%-O_2) (a), 3%-O_2 (b), 5%-O_2 (c), and 10%-O_2 (d) atmospheres

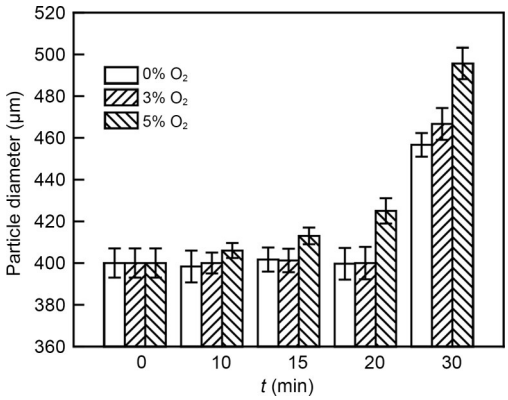

Fig. 4 Variations of particle size with time (*t*) when the IRN-97H cation-exchange resins were pyrolyzed at 450 ℃ in atmospheres with different oxygen contents

the reaction temperature to 520 ℃, the pyrolysis rate in the resin particles increased sharply. The pyrolysis gas generated in a short time burst the particles. In summary, when the pyrolysis temperature of resins is 400–500 ℃, the hole structure is easily formed in the particles, while the particle surface remains intact.

3.2.3 Effect of resin structure

Different types of cation-exchange resins have different crosslinking degrees and particle sizes. We used IR-120 gel cation-exchange resins to explore the effect of crosslinking degree on the resin pyrolysis behavior. We also selected the 001×7 gel cation-exchange resins to investigate the effect of particle size on the pyrolysis process. The TG curves of different resins in a 3%-O_2 atmosphere are shown in Fig. 6a. The pyrolysis weight-loss processes of different resins are similar and can be divided into two stages (Juang and Lee, 2002; Yang et al., 2014, 2017). The first is the decomposition and transformation of sulfonic acid groups at 300–500 ℃. The second is the stage of organic skeleton pyrolysis above 500 ℃ (Juang and Lee, 2002). However, there are some differences in the initial weight-loss temperature and rate in each stage. Compared with the thermal weight-loss process of IRN-97H resin, the weight-loss rate of IR-120 resin with the same particle size was higher under the same conditions. This indicates that the lower crosslinking degree makes the copolymer structure easier to destroy. The initial weight-loss temperature of 001×7 resin with an average particle size of 900 μm was higher. The weight-loss delay may be due to the decrease in the heat-transfer rate for the larger particle size.

Fig. 6 presents the internal morphologies of three pyrolyzed resins. The pyrolysis processes of IR-120

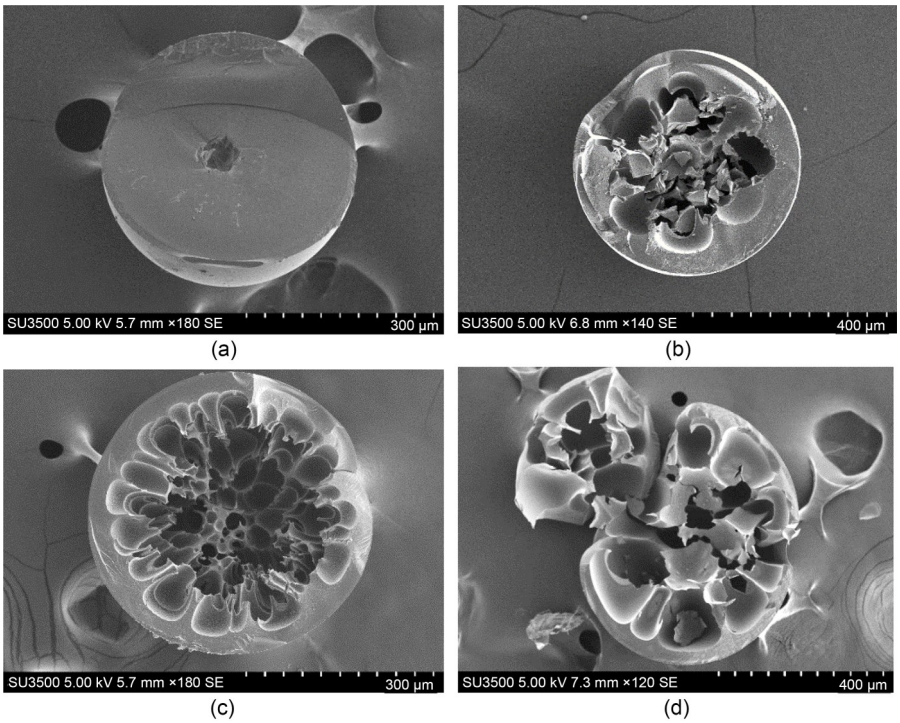

Fig. 5 Morphologies of IRN-97H cation-exchange resins pyrolyzed in a 3%-O_2 atmosphere at 400 ℃, 30 min (a), 450 ℃, 30 min (b), 500 ℃, 5 min (c), and 520 ℃, 5 min (d)

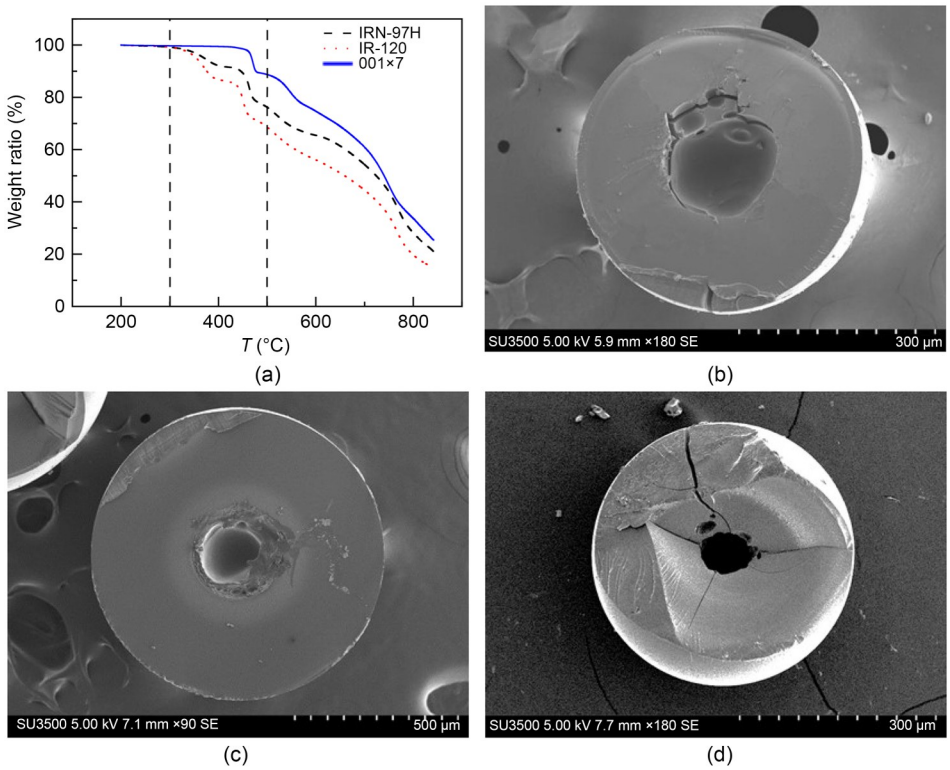

Fig. 6 TG curves of different resins in a 3%-O_2 atmosphere (a) and morphologies of IR-120 resin pyrolyzed for 10 min (b), 001×7 resin pyrolyzed for 20 min (c), and IRN-97H resin pyrolyzed for 10 min (d) at 450 °C in a 3%-O_2 atmosphere

resin and 001×7 resin were similar to that of IRN-97H resin. The reactions all started from the center of the resin particles. As the reaction time increased, the hole structure was formed inside the particles, while the outside surface remained intact. Compared with IRN-97H resin (Fig. 6d), the volume of the central hole was larger for IR-120 resin (Fig. 6b) when pyrolyzed for 10 min. This shows that the degree of pyrolysis is higher for IR-120 resin, since the resin with a lower crosslinking degree is more easily pyrolyzed. However, even though the 001×7 resin (Fig. 6c) was pyrolyzed for 20 min, only the central hole formed inside the particles. This may be due to the lower heat-transfer rate inside the resin with larger particle size, which would lead to a decrease in the reaction rate in the particles and an increase in the reaction time required to form holes.

The Co-doped resins and pure resins without metal ions were also pyrolyzed at 450 °C in a 3%-O_2 atmosphere for 30 min to investigate the influence of doped metal ions on their pyrolysis behaviors, and their interior structures are shown in Fig. S4 of the ESM. The pyrolysis behaviors of Co-doped resin and pure resin are similar to that of Cs^+-doped resin (Fig. 1e). The hole structure is formed inside the particle at 30 min, while the particle surface remains intact. These results show that the doped metal ions in the cation-exchange resin have little effect on the pyrolysis behavior of the resin.

In addition, the surface roughness of the particles may affect the heat and mass-transfer processes in the reaction, and then affect the pyrolysis behavior of the resin. The IRN-97H resins were sanded into rough particles to investigate the effect of surface roughness on their pyrolysis behavior. The surface morphologies of the particles before and after polishing, and the internal morphologies of the products pyrolyzed at 450 °C in a 3%-O_2 atmosphere for 20 min, are compared in Fig. 7. The pyrolysis behavior of rough resins was similar to that of smooth resins. A hole formed from the center of the particle at first and then developed into hole structures, while the surface remained unchanged. The volume of the holes in the pyrolysis products of rough resins was greater and the uniformity of hole distribution was less at 20 min when compared with the original smooth resins. This may be because the reaction gas was more likely to enter the interior of the rough particles, which would

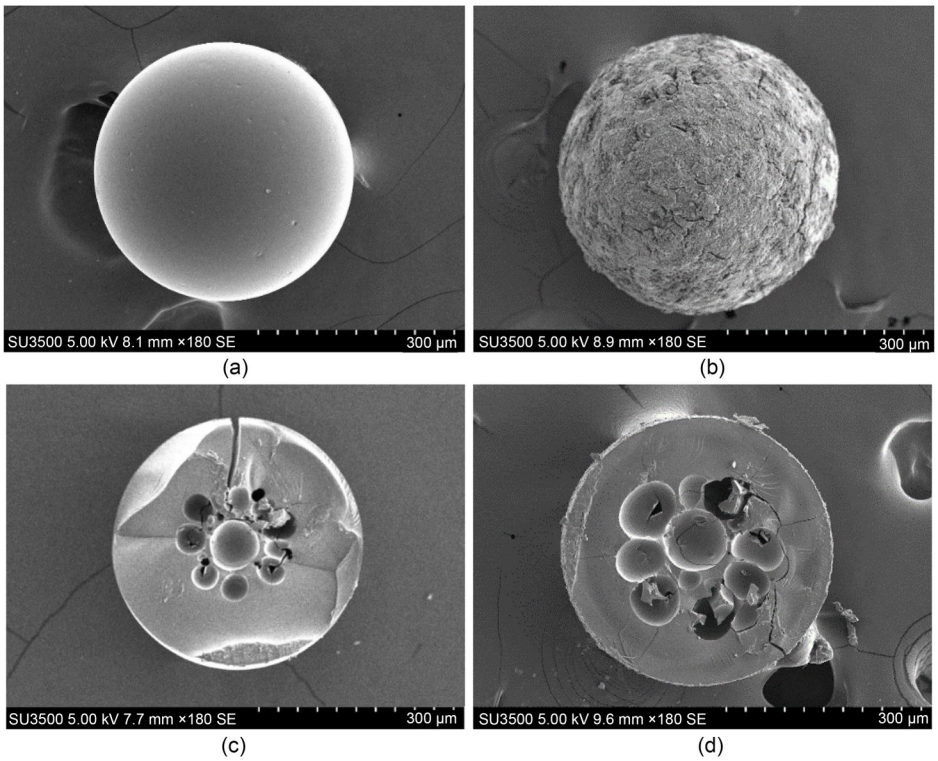

Fig. 7 Morphological comparison of the smooth resin (a) and rough resin (b), and the smooth resin's pyrolysis product (c) and rough resin's pyrolysis product (d) at 20 min

increase the degree of pyrolysis and lead to greater hole volume. Also, the sphericity degree of the rough resins was lower, resulting in anisotropy of the heat transfer inside the particles during the heating process, and the uniformity of hole distribution decreased.

Furthermore, the pore structure of the resin has a great influence on the mass transfer during the reaction. Ion-exchange resins can be divided into the gel type and macroreticular type. The latter has a larger pore size than the former. We selected D001 macroreticular cation-exchange resins with a crosslinking degree of 7% for pyrolysis at 450 ℃ in a 3%-O_2 atmosphere to explore the effect of pore structure. The morphologies of the products are shown in Fig. 8. Compared with the gel-type resin, the cut surface of the macroreticular resin was rougher, and the pores could be observed by SEM, indicating that the pore size was larger. At 10 min, the copolymer matrix inside the particle was pyrolyzed and many small holes were formed in the center area, while there was no obvious change on the particle surface. With a longer reaction time, the resin pyrolysis degree increased, and the holes expanded toward the edge of the particle. Both the number and volume of holes increased. The pyrolysis process of macroreticular resin can also be considered to start from the central region and expand to the edge of the particle, which follows the same pyrolysis law as the gel resin.

In summary, the cation-exchange resin always followed the same pyrolysis law at 400–500 ℃ with different parameters; the reaction always proceeded from the center of the particle to the surface. Specifically, the resin was pyrolyzed in the center of the particle to form the central hole at first, and then continued to be pyrolyzed around the central hole to form a uniformly distributed hole group. The holes expanded from the inside to the outside in this way until the particles burst. The volume and number of holes gradually increased, while the particle surface remained intact and there was no obvious change. We once thought that the resin pyrolysis process might follow the volume reaction model or shrinking core model just like other biomass pyrolysis and combustion processes (Sadhukhan et al., 2009; Oluoti et al., 2014; Yao et al., 2018), but in fact, the pyrolysis process of the cation-exchange resin starts from the center of the particle and then spreads around evenly, which is predictable. It does not follow any of the four classic non-catalytic

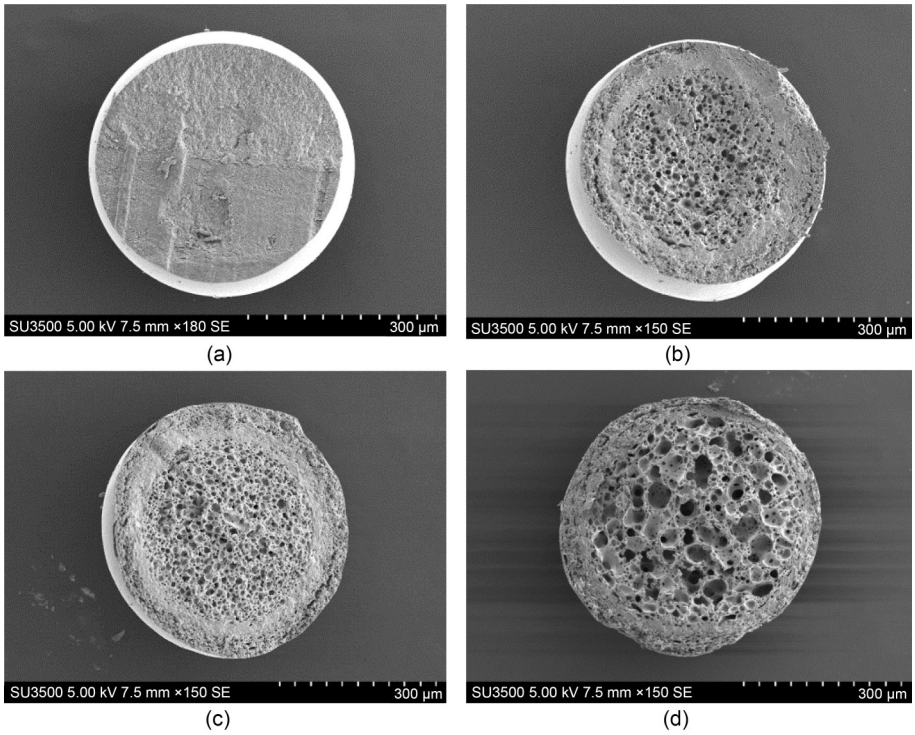

Fig. 8 Morphologies of D001 macroreticular resins (a) and products pyrolyzed at 450 ℃ in a 3%-O_2 atmosphere for 10 min (b), 20 min (c), and 30 min (d)

gas-solid reaction models. Therefore, we identified a novel non-catalytic gas-solid reaction and named it the central-hole expansion mode.

A schematic diagram of the central-hole expansion mode is presented in Fig. 9. The reaction gas coats the solid surface to form a gas film and enters the interior of the solid during the reaction. The reaction starts from the center of the particle, and a hole is first formed there. Subsequently, the volume of the central hole gradually increases, and the surrounding sites continue to react to form a uniformly distributed hole group. As the reaction progresses, both the number and volume of holes inside the particle increase. Finally, a hollow particle with many holes inside is formed but the surface remains intact. In this process, the particle size also gradually increases. When the volume of the particle expands to a certain extent, it will eventually break up and form fragments.

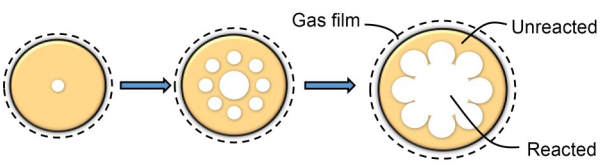

Fig. 9 Schematic diagram of the central-hole expansion mode

3.3 Formation mechanism of the central-hole expansion mode

3.3.1 Pyrolysis of the copolymer matrix

The pyrolysis process of cation-exchange resin can be divided into two stages. The first stage is decomposition and transformation of the sulfonic acid groups, which are bonded to the copolymer matrix polystyrene-divinylbenzene (St-DVB) and release part of the SO_2, as shown in Eq. (1). The second stage is pyrolysis of the organic skeleton to form hydrocarbons and residue (Eq. (2)) (Yang et al., 2017).

$$\begin{aligned}&(\text{St-DVB-SO}_3\text{H})_n \rightarrow (\text{St-DVB-SO}_2\text{-})_n + \\ &(\text{St-DVB-S-})_n + (\text{St-DVB})_n + \text{SO}_2, \end{aligned} \quad (1)$$

$$\begin{aligned}&(\text{St-DVB-SO}_2\text{-})_n + (\text{St-DVB-S-})_n + \\ &(\text{St-DVB})_n \rightarrow \text{C}_x\text{H}_y + \text{SO}_2 + \text{H}_2\text{O} + \text{Residue}. \end{aligned} \quad (2)$$

In order to investigate the effect of the sulfonic-acid group reaction on the central-hole expansion mode and clarify the hole-formation conditions, we also

studied the pyrolysis of St-DVB resin particles. The TG and DTG curves of St-DVB resins in different atmospheres are presented in Fig. 10a. It can be seen that there was only one weight-loss peak in the pyrolysis of St-DVB resins, indicating that the polystyrene cross-linked divinylbenzene structure was directly pyrolyzed, and that the pyrolysis degree reached 100% without solid residue. In a nitrogen atmosphere, the St-DVB resins began to reduce in weight at about 400 °C and were pyrolyzed completely at around 480 °C. In the 3%-O_2 atmosphere, the initial weight-loss temperature was about 300 °C, 100 °C lower than that in the nitrogen atmosphere. This indicated that oxygen has a strong promotion effect on the pyrolysis of St-DVB resins. The St-DVB resins were pyrolyzed at 300 °C in the 3%-O_2 atmosphere, and the morphologies of the initial particles and pyrolysis products are shown in Fig. 10. The surface of the initial St-DVB resin particle was smooth, while the cut surface was rough. When pyrolyzed for 20 min, the particle surface was damaged, and particle size decreased from the initial 405 to 345 μm. In addition, no holes were formed inside the particle and there was no significant change of the interior compared to the original particle, indicating that no reaction occurred inside the St-DVB resin. The results show that the pyrolysis process of St-DVB resins starts from the surface and proceeds from the outside to the inside, accompanied by a decrease in particle volume. This process follows the shrinking core model, one of the classic non-catalytic gas-solid reaction models. Therefore, we speculate that the central-hole expansion mode in the pyrolysis of cation-exchange resins is related to the sulfonic acid groups.

3.3.2 Decomposition and transformation of sulfonic acid groups

Fig. 11 shows the TG and DTG curves and heat-flow curve of IRN-97H resins in the 3%-O_2 atmosphere. The sulfonic acid groups (-SO_3M) easily decomposed to form SO_2 and sulfone groups (-SO_2-) at low temperatures (300–410 °C). At high temperatures (410–500 °C), sulfonic acid groups transformed into sulfone groups (-SO_2-) and sulfur bonds (-S-), and the formed sulfone groups were further converted into sulfur bonds. The sulfone groups and sulfur bonds cross-linked with the St-DVB copolymer matrix to form organic sulfur structures such as diphenyl sulfone and phenyl sulfide (Matsuda et al., 1987; Chun et al., 1998). The organic sulfur structures had strong thermal stability (Singare et al., 2010; Asfaw et al., 2016) and were gradually destroyed only when the temperature was higher than 500 °C. In contrast with

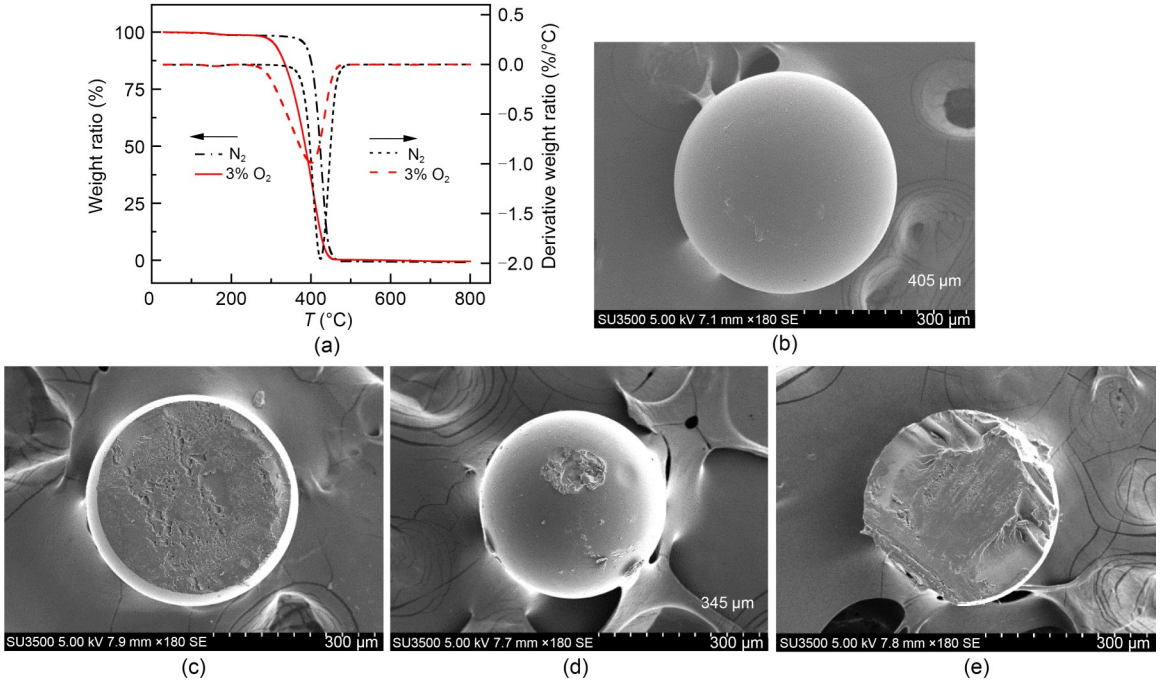

Fig. 10 TG and DTG curves (a), original morphologies (b (surface) and c (cut surface)), and product morphologies (d (surface) and e (cut surface)) of the St-DVB resins pyrolyzed at 300 °C in a 3%-O_2 atmosphere for 20 min

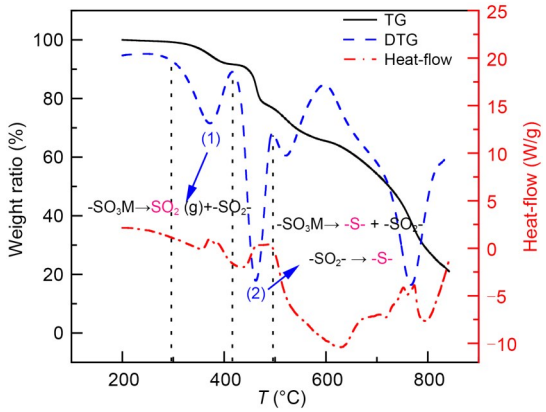

Fig. 11 TG and DTG curves and heat-flow curve of IRN-97H resin in the 3%-O_2 atmosphere

the pyrolysis of St-DVB (Fig. 10), the reason why the cation-exchange resins still could not be pyrolyzed completely at 800 ℃ was simply the formation of the organic sulfur cross-linked structures, which hindered pyrolysis of the copolymer matrix. Moreover, it can be seen from the heat-flow curve that the reaction of the sulfonic acid groups and pyrolysis of the organic skeleton were both strong endothermic processes.

Fig. 12 shows the S 2p XPS spectra of the particle surface of raw resins and pyrolysis products obtained with 450 ℃ and 3%-O_2 atmosphere at different times. The binding-energy values at 169.6, 168.8, 168.2, and 164.0 eV can be assigned to sulfates, sulfonic acid groups, sulfones, and phenyl sulfide, respectively (Matsuda et al., 1987; Hu et al., 2014; Hou et al., 2018). In the pyrolysis of cation-exchange resins, the sulfonic acid groups on the particle surface transformed into sulfone groups and sulfur bonds at 10 min and then cross-linked with the copolymer matrix to form organic sulfur structures such as diphenyl

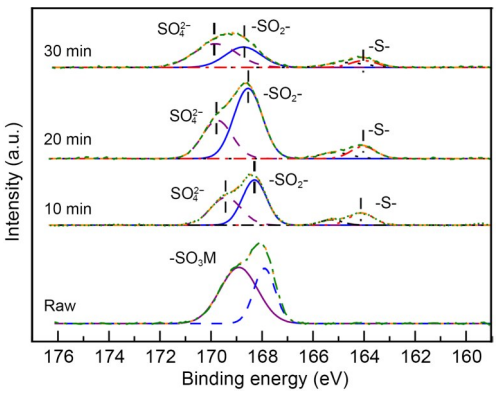

Fig. 12 S 2p XPS spectra of the surface of raw resins and pyrolysis products obtained at 450 ℃ in a 3%-O_2 atmosphere

sulfone and phenyl sulfide. Some sulfurs in the sulfonic acid groups were even converted into the final stable form, sulfates. The relative area of the sulfate peak gradually increased with the reaction time, indicating that part of the unstable sulfone groups and sulfur bonds gradually transformed into sulfates, while the stable organic sulfur structures always existed. Thus, the organic sulfur structures formed on the particle surface were difficult to destroy in the subsequent pyrolysis process, resulting in the intact particle surface.

The formation of holes inside the resin particles may be due to the different reaction processes of sulfonic acid groups on the surface and interior. Researchers have found that when biomass particles at normal temperatures are placed in a high-temperature environment for reaction, the surface temperature of the particles increases instantaneously and reaches the ambient temperature within a few seconds (Gómez et al., 2015; Chen et al., 2018). However, there is a hysteresis in the temperature change inside the particles due to the effect of the heat-transfer process and endothermic reaction, resulting in a certain temperature difference between the surface and interior of the particles in the initial stage of the reaction. The pyrolysis of resin studied in this work followed the same course. When the resin particles at normal temperature were placed in 450-℃ environment for pyrolysis, the surface temperature of the particles rose to 450 ℃ in a very short time. However, it took a certain amount of time for the heat to transfer from the particle surface to the interior. More importantly, both the reaction of sulfonic acid groups and pyrolysis of the organic skeleton are strongly endothermic reactions. Thus, the temperature inside the particles at the initial reaction stage is always below 450 ℃. During this stage, the difference in temperature between the surface and interior of the particles leads to different reaction processes of the sulfonic acid groups, which affects the pyrolysis behavior inside and on the surface of the particles.

We preliminarily simulated the temperature change of the resin particles during the initial reaction stage with COMSOL Multiphysics. In the simulation, a sphere geometry with a diameter of 400 μm was established, and an area with a diameter of 40 μm was added in the center of the sphere as a volume endothermic source to represent the endothermic reaction. The thermophysical properties of the resin particle

and boundary conditions in the simulation are listed in Table S1 of the ESM. The heat-transfer module used in the simulation was heat transfer in solids and the heat transfer between the particle surface and environment was set as natural convection heat transfer (Eq. (S1) of the ESM). The interior of the particle was set as a combined heat transfer of heat conduction and endothermic source (Eqs. (S2) and (S3) of the ESM). The temperature changes on the surface and in the center of the resin particle are shown in Fig. S5 of the ESM. The temperature of the particle surface quickly rose to the environment temperature (450 ℃) within 5 s, so most of the sulfonic acid groups were transformed. However, due to heat conduction, there was a hysteresis in the temperature rise in the center of the particle. During this 5-s period, the interior and surface of the particle began to react, and the endothermic source was formed, causing the temperature of the particle center to stabilize at about 380 ℃ in the early stage of the pyrolysis reaction; this induced decomposition of the sulfonic acid groups inside the particle.

We assumed both the decomposition and transformation reactions of the sulfonic acid groups to be first-order reactions and analyzed the kinetics of the decomposition and transformation of the sulfonic acid groups by the Flynn-Ozawa method. The equal conversion not only reduced the influence of the heating rate, but also did not involve the reaction mechanism function (Vyazovkin et al., 2011; Yang et al., 2014). The mechanism function $f(\alpha)$ and kinetic parameters are listed in Table 2. To compare the reaction rate of the two processes, we substituted the peak temperature of sulfonic-acid-group decomposition at 380 ℃ and that of transformation at 450 ℃ into the Arrhenius kinetic equations of the two processes. The relationship between conversion α and time t was obtained by integration (Fig. S6 of the ESM). The decomposition and transformation processes of sulfonic acid groups are both fast reactions, and the reaction rate of decomposition is faster. Although the temperature of the decomposition process is lower, its conversion was already higher than 90% at 30 s, and conversion above 90% in the transformation process required at least 65 s. Therefore, from the perspective of numerical simulation and kinetics analysis, it appears that in the early stage of the resin pyrolysis reaction, the sulfonic acid groups inside the resin particles mainly decompose at low temperatures. The decomposed sulfonic acid groups will fall off the copolymer matrix to form SO_2. The copolymer matrix without sulfonic acid groups can be completely pyrolyzed under the reaction conditions (Fig. 10), and the release rate of volatile components from the resin's matrix is greater than its diffusion rate in the particle, resulting in the formation of holes.

In order to verify the above conjecture, we immersed the product particles formed by pyrolysis in a 450-℃, 3%-O_2 atmosphere for 30 min in 1-mol/L KOH solution, and then crushed them to release the acid gas inside to be adsorbed by the KOH solution. The anion component in the solution was analyzed by ion chromatograph. The chromatographic peak with a residence time of 9.91 min was SO_3^{2-}, and the peak with a residence time of 10.88 min was SO_4^{2-} (Fig. S7 of the ESM). The SO_4^{2-} in the solution was converted from the sulfonic acid group during the pyrolysis of cation-exchange resin, but the sulfonic acid group was not converted to SO_3^{2-}. Therefore, SO_3^{2-} is most likely to be produced by the reaction of SO_2 inside the product particles with the KOH solution, indicating that during the pyrolysis process of the resin, SO_2 will be generated inside the particles, corresponding to the decomposition reaction of the sulfonic acid group.

Thus, the main reason for the formation of holes in the central-hole expansion mode is that the reaction path of sulfonic acid groups inside the resin particles is different from that on the surface. It requires an environmental reaction temperature higher than the transformation temperature of sulfonic acid groups (410 ℃) to ensure that transformation of sulfonic acid groups occurs on the surface. Meanwhile, in order to prevent the fracture of the particle surface caused by

Table 2 Kinetics of decomposition and transformation of sulfonic acid groups in the pyrolysis of resins

Reaction step	Temperature, T (℃)	Mechanism function, $f(\alpha)$	Activation energy, E (kJ/mol)	Pre-exponential factor, A (s^{-1})	Reaction-rate equation
Decomposition of -SO_3M	300–410	$1-\alpha$	188.4	1.0×10^{14}	$\frac{d\alpha}{dt}=f(\alpha)Ae^{-\frac{E}{RT}}$
Transformation of -SO_3M	410–500	$1-\alpha$	317.2	3.1×10^{21}	

R is the molar gas constant

destruction of the organic sulfur structures, the reaction temperature should also be lower than the pyrolysis temperature of the organic skeleton, which is 500 ℃. In summary, the theoretical temperature range for the occurrence of central-hole expansion mode in the pyrolysis of cation-exchange resins should be 410–500 ℃.

4 Conclusions

In this study, we identified a novel non-catalytic gas-solid reaction, which we call the central-hole expansion mode, while investigating the pyrolysis process of strongly acidic cation-exchange resins. In this mode, the pyrolysis reaction starts from the center of the resin particle to form a central hole. Then the resin continues to be pyrolyzed around the central hole to form a uniformly distributed hole group. The holes expand from the inside to the outside in this way. The volume and number of holes gradually increase, and the particle size also increases, while the particle surface remains intact and there is no externally obvious change. The cation-exchange resins always follow the same pyrolysis law at 400–500 ℃ with different oxygen-content atmospheres, different crosslinking degrees and particle sizes, different doped metal ions, and different surface roughness and pore structures. We also preliminarily investigated the formation mechanism of the central-hole expansion mode, and found that it is mainly related to the reaction path of sulfonic acid groups. In the early stage of the pyrolysis reaction, there is a certain temperature difference between the surface and interior of the particle, which leads to the difference in the reaction paths and reaction rates of the sulfonic acid groups and copolymer matrices inside and outside the particle. The sulfonic acid groups on the surface of the resin particles mainly transform into sulfone groups and sulfur bonds at high temperatures (410–500 ℃), and these cross-link with the copolymer matrix to form stable organic sulfur structures, resulting in an intact particle surface. The sulfonic acid groups inside the resin particles primarily decompose at a relatively low temperature (<410 ℃) and fall off the copolymer matrix to form SO_2. The copolymer matrix without sulfonic acid groups can be completely pyrolyzed to form holes. The central-hole expansion mode in this study may provide guidance for the verification and development of non-catalytic gas-solid reaction models due to its regular reaction process and predictable reaction sites.

Acknowledgments

This work is supported by the Joint Funds of the National Natural Science Foundation of China (No. U21B2095), the Major Research Project of National Natural Science Foundation of China (No. 91834303), and the Science Fund for Creative Research Groups of National Natural Science Foundation of China (No. 61621002).

Author contributions

Zheng-liang HUANG and Yao YANG designed the research. Zheng-liang HUANG, Yun-bo YU, and Qi SONG processed the corresponding data. Yun-bo YU and Qi SONG wrote the first draft of the manuscript. Yao YANG, Jing-yuan SUN, and Jing-dai WANG helped to organize the manuscript. Yao YANG and Yong-rong YANG revised and edited the final version.

Conflict of interest

Zheng-liang HUANG, Yun-bo YU, Qi SONG, Yao YANG, Jing-yuan SUN, Jing-dai WANG, and Yong-rong YANG declare that they have no conflict of interest.

References

Amutio M, Lopez G, Aguado R, et al., 2012. Kinetic study of lignocellulosic biomass oxidative pyrolysis. *Fuel*, 95:305-311. https://doi.org/10.1016/j.fuel.2011.10.008

Asfaw HD, Younesi R, Valvo M, et al., 2016. Boosting the thermal stability of emulsion-templated polymers via sulfonation: an efficient synthetic route to hierarchically porous carbon foams. *ChemistrySelect*, 1(4):784-792. https://doi.org/10.1002/slct.201600139

Bach QV, Trinh TN, Tran KQ, et al., 2017. Pyrolysis characteristics and kinetics of biomass torrefied in various atmospheres. *Energy Conversion and Management*, 141:72-78. https://doi.org/10.1016/j.enconman.2016.04.097

Bava YB, Geronés M, Giovanetti LJ, et al., 2019. Speciation of sulphur in asphaltenes and resins from Argentinian petroleum by using XANES spectroscopy. *Fuel*, 256:115952. https://doi.org/10.1016/j.fuel.2019.115952

Chen T, Ku X, Lin JZ, et al., 2018. New pyrolysis model for biomass particles in a thermally thick regime. *Energy & Fuels*, 32(9):9399-9414. https://doi.org/10.1021/acs.energyfuels.8b01261

Chen YJ, Jing L, Li XL, et al., 2006. Suppressed anion chromatography using mixed zwitter-ionic and carbonate eluents. *Journal of Chromatography A*, 1118(1):3-11. https://doi.org/10.1016/j.chroma.2005.12.074

Chun UK, Choi K, Yang KH, et al., 1998. Waste minimization pretreatment via pyrolysis and oxidative pyroylsis of organic ion exchange resin. *Waste Management*, 18(3):183-196. https://doi.org/10.1016/S0956-053X(98)00020-8

Gómez MA, Porteiro J, Patiño D, et al., 2015. Fast-solving thermally thick model of biomass particles embedded in a CFD code for the simulation of fixed-bed burners. *Energy Conversion and Management*, 105:30-44. https://doi.org/10.1016/j.enconman.2015.07.059

Homma S, Ogata S, Koga J, et al., 2005. Gas–solid reaction model for a shrinking spherical particle with unreacted shrinking core. *Chemical Engineering Science*, 60(18): 4971-4980. https://doi.org/10.1016/j.ces.2005.03.057

Hou JL, Ma Y, Li SY, et al., 2018. Transformation of sulfur and nitrogen during Shenmu coal pyrolysis. *Fuel*, 231:134-144. https://doi.org/10.1016/j.fuel.2018.05.046

Hu HY, Fang Y, Liu H, et al., 2014. The fate of sulfur during rapid pyrolysis of scrap tires. *Chemosphere*, 97:102-107. https://doi.org/10.1016/j.chemosphere.2013.10.037

Juang RS, Lee TS, 2002. Oxidative pyrolysis of organic ion exchange resins in the presence of metal oxide catalysts. *Journal of Hazardous Materials*, 92(3):301-314. https://doi.org/10.1016/S0304-3894(02)00025-0

Matsuda M, Funabashi K, Yusa H, et al., 1987. Influence of functional sulfonic acid group on pyrolysis characteristics for cation exchange resin. *Journal of Nuclear Science and Technology*, 24(2):124-128. https://doi.org/10.1080/18811248.1987.9735785

Oluoti KO, Richards T, Doddapaneni TRK, et al., 2014. Evaluation of the pyrolysis and gasification kinetics of tropical wood biomass. *BioResources*, 9(2):2179-2190. https://doi.org/10.15376/biores.9.2.2179-2190

Petersen EE, 1957. Reaction of porous solids. *AIChE Journal*, 3(4):443-448. https://doi.org/10.1002/aic.690030405

Ramachandran PA, Doraiswamy LK, 1982. Modeling of noncatalytic gas-solid reactions. *AIChE Journal*, 28(6):881-900. https://doi.org/10.1002/aic.690280602

Ren QQ, Zhao CS, 2012. NO_x and N_2O precursors from biomass pyrolysis: nitrogen transformation from amino acid. *Environmental Science & Technology*, 46(7):4236-4240. https://doi.org/10.1021/es204142e

Sadhukhan AK, Gupta P, Saha RK, 2009. Modelling of pyrolysis of large wood particles. *Bioresource Technology*, 100(12):3134-3139. https://doi.org/10.1016/j.biortech.2009.01.007

Sadhukhan AK, Gupta P, Saha RK, 2010. Modelling of combustion characteristics of high ash coal char particles at high pressure: shrinking reactive core model. *Fuel*, 89(1): 162-169. https://doi.org/10.1016/j.fuel.2009.07.029

Safari V, Arzpeyma G, Rashchi F, et al., 2009. A shrinking particle—shrinking core model for leaching of a zinc ore containing silica. *International Journal of Mineral Processing*, 93(1):79-83. https://doi.org/10.1016/j.minpro.2009.06.003

Shen DK, Gu S, Jin BS, et al., 2011. Thermal degradation mechanisms of wood under inert and oxidative environments using DAEM methods. *Bioresource Technology*, 102(2):2047-2052. https://doi.org/10.1016/j.biortech.2010.09.081

Singare PU, Lokhande RS, Madyal RS, 2010. Thermal degradation studies of polystyrene sulfonic and polyacrylic carboxylic cationites. *Russian Journal of General Chemistry*, 80(3):527-532. https://doi.org/10.1134/s1070363210030266

Szekely J, Propster M, 1975. A structural model for gas solid reactions with a moving boundary-VI: the effect of grain size distribution on the conversion of porous solids. *Chemical Engineering Science*, 30(9):1049-1055. https://doi.org/10.1016/0009-2509(75)87006-0

Trubetskaya A, Leahy JJ, Yazhenskikh E, et al., 2019. Characterization of woodstove briquettes from torrefied biomass and coal. *Energy*, 171:853-865. https://doi.org/10.1016/j.energy.2019.01.064

Uhde G, Hoffmann U, 1997. Noncatalytic gas-solid reactions: modelling of simultaneous reaction and formation of surface with a nonisothermal crackling core model. *Chemical Engineering Science*, 52(6):1045-1054. https://doi.org/10.1016/S0009-2509(96)00443-5

Vyazovkin S, Burnham AK, Criado JM, et al., 2011. ICTAC kinetics committee recommendations for performing kinetic computations on thermal analysis data. *Thermochimica Acta*, 520(1-2):1-19. https://doi.org/10.1016/j.tca.2011.03.034

Wen CY, 1968. Noncatalytic heterogeneous solid-fluid reaction models. *Industrial & Engineering Chemistry*, 60(9): 34-54. https://doi.org/10.1021/ie50705a007

Yagi S, Kunii D, 1955. Studies on fluidized-solids reactors for particles with decreasing diameters. *Chemical Engineering*, 19(10):500-506 (in Janpanese). https://doi.org/10.1252/kakoronbunshu1953.19.500

Yang HC, Lee MW, Hwang HS, et al., 2014. Study on thermal decomposition and oxidation kinetics of cation exchange resins using non-isothermal TG analysis. *Journal of Thermal Analysis and Calorimetry*, 118(2):1073-1083. https://doi.org/10.1007/s10973-014-3853-9

Yang HC, Lee SY, Choi YC, et al., 2017. Thermokinetic analysis of spent ion-exchange resins for the optimization of carbonization reactor condition. *Journal of Thermal Analysis and Calorimetry*, 127(1):587-595. https://doi.org/10.1007/s10973-016-5817-8

Yao X, Yu QB, Han ZR, et al., 2018. Kinetic and experimental characterizations of biomass pyrolysis in granulated blast furnace slag. *International Journal of Hydrogen Energy*, 43(19):9246-9253. https://doi.org/10.1016/j.ijhydene.2018.03.173

Yoshioka T, Motoki T, Okuwaki A, 2001. Kinetics of hydrolysis of poly (ethylene terephthalate) powder in sulfuric acid by a modified shrinking-core model. *Industrial & Engineering Chemistry Research*, 40(1):75-79. https://doi.org/10.1021/ie000592u

Electronic supplementary materials

Figs. S1–S7, Table S1, Eqs. (S1)–(S3)